Organic Electronics 13 (2012) 1479–1485

Contents lists available at SciVerse ScienceDirect

Organic Electronics

journal homepage: www.elsevier.com/locate/orgel

# Phthalonitrile based fluorophores as fluorescent dopant emitters in deep-blue OLEDs: Approaching the NTSC standard for blue

Brett A. Kamino [a], Yi-Lu Chang [b], Zheng-Hong Lu [b], Timothy P. Bender [a,*]

[a] Department of Chemical Engineering and Applied Chemistry, The University of Toronto, 200 College St., Toronto, Ontario, Canada M5S 3E5
[b] Department of Materials Science and Engineering, The University of Toronto, 184 College St., Toronto, Ontario, Canada M5S 3E4

ARTICLE INFO

*Article history:*
Received 31 January 2012
Received in revised form 28 March 2012
Accepted 15 April 2012
Available online 27 April 2012

*Keywords:*
Phthalonitrile
Deep-blue
Fluorescent
OLED

ABSTRACT

Unprecedented phthalonitrile based fluorophores are reported and studied for incorporation into organic light emitting diodes. The phthalonitriles were obtained using a very simple synthetic procedure and were found to be highly fluorescent with quantum yields approaching unity; they are also thermally stable and electrochemically active. When incorporated into OLEDs as fluorescent dopants, the resulting devices have good device efficiencies and emit in the deep-blue area of the spectrum with CIE coordinates that are close to the NTSC standard for blue.



## 1. Introduction

Organic light emitting diodes (OLEDs) are a promising technology for full-colour, large area display technology [1]. Such displays typically rely on the use of the red, green, blue (RGB) colour space which requires separate emission from red, green, and blue materials/OLEDs. Currently, highly efficient phosphorescent OLEDs emitting red and green light are well-known and can achieve internal quantum efficiencies approaching unity. However, the development of high-efficiency blue OLEDs with Commission Internationale de l'éclairage (CIE) [2] coordinates matching the NTSC colour standard for blue ($CIE_x$ = 0.14, $CIE_y$ = 0.08) [3] has proven more difficult and remains a current challenge for display technology. Blue phosphorescent devices have been studied extensively and a number of non-saturated blue or sky-blue devices are well known [4,5]. While high efficiencies have been achieved these technologies still have many disadvantages for display technologies including poor colour saturation and extremely short operational lifetimes [6]. Improvements in colour saturation for these devices has recently been developed through the engineering of better host materials [7,8] and phosphorescent emitting materials [9]. These devices have impressive performance but phosphorescent devices are still largely limited to $CIE_y$ coordinates of $\geqslant$0.15 and issues with the stability of high energy phosphorescent emitters remain. Therefore, there is still room for further improvement in colour saturation and stability by engineering materials that can more closely match the standard for blue colour in display technology.

One alternative approach to this problem has been to combine a blue fluorescent dopants with red and green phosphorescent dopants to achieve full colour displays [10,11]. While fluorescent blue emitting materials are inherently less efficient due to only being able to harvest singlet excitons/electron–hole pairs, they are better able to achieve deep-blue emission while maintaining high photoluminescent efficiencies and chemical stability. Because of this, there is a strong interest in developing high-efficiency, deep-blue fluorescent OLEDs that can approach the NTSC colour standard for blue. In regards to material design however, there are relatively few classes of materials that satisfy these requirements. The majority of these are based on a limited number of structural

* Corresponding author.
*E-mail address:* tim.bender@utoronto.ca (T.P. Bender).

1566-1199/$ - see front matter © 2012 Elsevier B.V. All rights reserved.
http://dx.doi.org/10.1016/j.orgel.2012.04.014

themes, including: styrlbiphenyls [12–15], acenes [16,17], group III metal complexes [18] and phenylquinolines [19]. Given this limited pool of deep-blue emitting groups, there exists a need to identify additional molecular structures which emit deep-blue light.

In this paper, we disclose an unprecedented pair of highly-emissive phthalonitrile based blue emitters and establish their utility in deep-blue OLED devices that closely match the NTSC standard for blue.

## 2. Experimental

### 2.1. General methods and procedures

Chemicals were purchased and used without further purification using standard laboratory methods. NMR spectra were collected at 25 °C at a field strength of 400 MHz. Chemical shifts are referenced to residual solvent signals. High resolution mass spectroscopy (HRMS) was obtained using an AccuTOF mass spectrometer (JEOL USA Inc., Peabody, MA) with a DART-SVP ion source (Ionsense Inc., Saugus, MA) using He gas. Electrochemistry was performed using a standard three electrode setup. A platinum disk was used as the working electrode while a platinum wire was used as a counter electrode. All data is corrected to the internal redox standard of decamethylferrocene [20] and numbers are referenced to Ag/AgCl. Thermogravimetric analysis (TGA) was performed at ramp rate of 10 °C/min under $N_2$.

Density functional theory calculations were performed using Spartan '06 for windows. Geometry optimizations were carried out using the Becke–Lee–Yang–Parr exchange correlation function [21] with a 6-31G(D) basis set.

The OLEDs were fabricated in a cluster tool (Kurt J. Lesker LUMINOS®) under a base pressure of $\sim 10^{-8}$ Torr on pre-patterned indium tin oxide (ITO) coated glass with a thickness of 1.1 mm. Prior to loading, the ITO was cleaned using standard solvents. Subsequently, a $MoO_3$ layer was deposited on top to obtain a high work function and facilitate hole injection into CBP. All organic layers were deposited in a dedicated chamber, whereas the cathode, consisting of LiF(1 nm)/Al(100 nm), was evaporated in a separate chamber without breaking vacuum. The active area of each device was 2 $mm^2$ as measured by an optical microscope. The EQE and power efficiency were measured using an integrating sphere with a silicon photodiode with NIST traceable calibration. The electroluminance (EL) spectra were measured using an Ocean Optics USB4000 spectrometer. All measurements were done in air with 3 s dwell time between each data point.

### 2.2. Synthesis of *1* and *2*

Synthesis of **1**: Tetrachlorophthalonitrile (1.00 g, 3.76 mmol), catechol (1.03 g, 9.38 mmol), potassium carbonate (1.30 g, 9.38 mmol), and dimethylformamide (20 mL) were heated to 100 °C under argon for 1 h. After cooling to room temperature, the solids were filtered and washed with water (100 mL) then methanol (50 mL). The collected solids were dried under vacuum to yield a fine white powder (1.20 g, 94% yield). $^1$H NMR (400 MHz, $CDCl_3$): $\delta$ 7.08–7.01 (m). HRMS (DART) [M+$NH_4$] calcd for $C_{20}H_{12}N_3O_4$ 358.0828, found 358.0822. Elemental Analysis calcd for (%) $C_{20}H_8N_2O_4$: C 70.59, H 2.37, N 8.23. Found: C 70.56, H 2.33, N 8.31.

Synthesis of **2**: Tetrachlorophthalonitrile (3.00 g, 11.3 mmol), 2,3-dihydroxynaphthalene (4.52 g, 28.2 mmol), potassium carbonate (3.90 g, 28.2 mmol), and dimethylformamide (60 mL) were heated to 100 °C under argon for 5 h. The cooled solids were collected by filtration and washed with water (200 mL), methanol (200 mL), then dichloromethane (50 mL), in that order. The resulting solids were dried under vacuum to yield a fine white powder (4.74 g, 95% yield). $^1$H NMR (400 MHz, $CDCl_3$): $\delta$ 7.74 (q, $J$ = 3.52 Hz, 4H), 7.51 (d, $J$ = 7.91 Hz, 4H), 7.45 (q, $J$ = 3.22 Hz, 4H). HRMS (DART) [M+H] calcd for $C_{28}H_{13}N_2O_4$ 441.0875, found 441.0876. Elemental Analysis calcd for (%) $C_{28}H_{12}N_2O_4$: C 76.36, H 2.75, N 6.36. Found: C 75.98, H 3.00, N 6.29.

## 3. Results and discussion

The inspiration for this study came from the description of **1** (Scheme 1) in a patent concerning new phthalonitriles for the synthesis of phthalocyanines [22] wherein no mention of the fluorescent or other optical properties was included. Upon repeating the described synthesis, we discovered that compound **1** was highly fluorescent even when photo-excited with a simple laboratory UV lamp. We also decided to synthesize a structural variant in the form of compound **2** as the reagent was commercially available (Scheme 1). Both phthalonitriles contain an extended π-electron system through two [1,4] benzodioxin linkages to yield highly conjugated and planar compounds (as shown by DFT calculations, Fig. 1).

The syntheses rely on nucleophilic aromatic substitution of tetrachlorophthalonitrile with the appropriate aromatic 1,2-diol in dimethylformamide along with stoichiometric quantities of potassium carbonate. Both syntheses proceeded rapidly and cleanly from commercially available

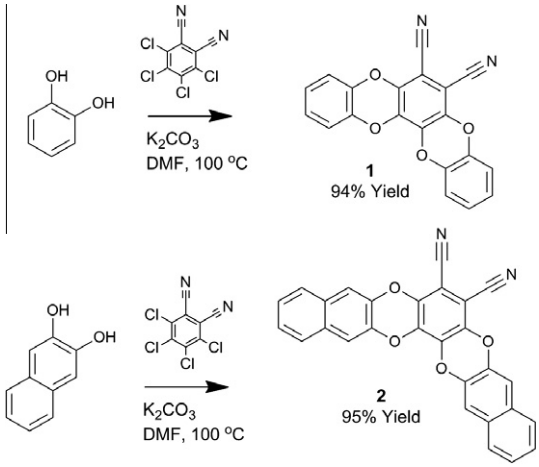


**Scheme 1.** Synthetic pathways towards phthalonitriles **1** and **2**.

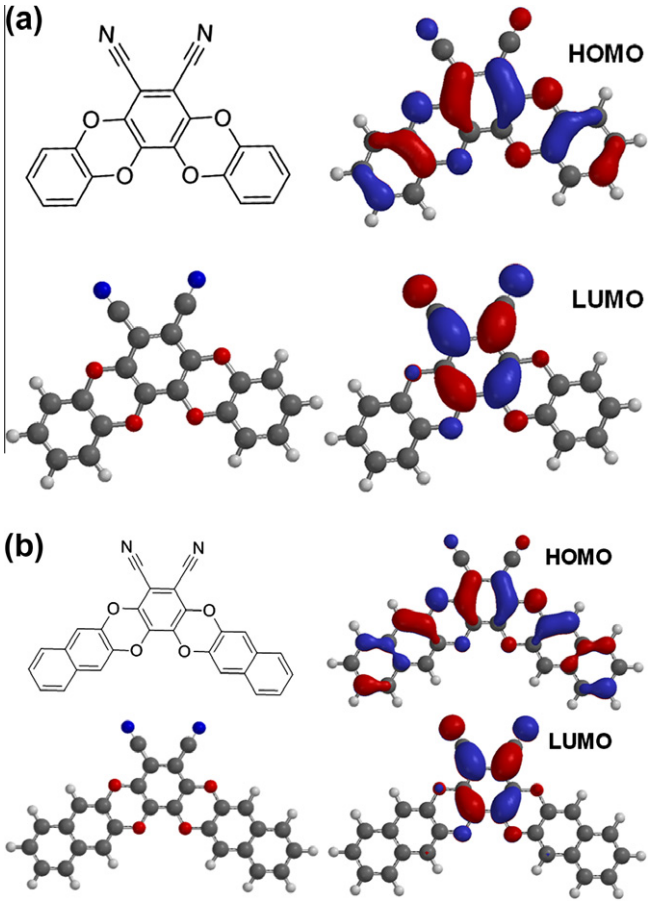


**Fig. 1.** Geometry optimized structure for (a) compound **1** and (b) compound **2** and their predicted HOMO and LUMO distributions.

starting materials to produce the desired products in high yields. Purification was rapidly achieved by simply filtering the pure product and washing with solvent. The resulting materials were isolated as insoluble white powders and we did not detect the formation of regioisomers. Despite the facile workup procedure, exceptionally high purities were achieved for both compounds without the need for subsequent purification steps. Structural determination and purity was achieved through elemental analysis and high-resolution mass spectrometry. Additionally, $^{1}$H NMR of the compounds is reported. Unfortunately, the poor solubility of the compounds inhibited us from acquiring $^{13}$C NMR data.

The photophysical properties of each compound were explored through solution UV–VIS absorbance and photoluminescence measurements in tetrahydrofuran (Fig. 2). Additionally, solid-state photoluminescence measurements were taken from vacuum deposited films. All of this data is summarized in Table 1. From this data, we observe that each compound emits in the deep-blue area of the spectrum in both solution and in the solid-state. Interestingly, both the onset of absorbance and the solution emission peak for **1** are slightly red shifted compared to **2** (~5 nm) in solution. This is somewhat surprising considering the greater conjugation length of **2** versus **1** which would normally facilitate the opposite trend as seen in a series of acenes (e.g. benzene, naphthalene, anthracene). As well, ground-state conjugation throughout each structure is confirmed by the DFT modelling results (Fig. 1) further supporting this prediction. We believe that this deviation from the expected behaviour may be due to the nature of conjugation throughout each molecule. The presence of planar oxygen atoms in these structures leads to hyperconjugation between the peripheral phenyl units and the central phthalonitrile core through the oxygen atoms. This less than perfect delocalization across the structure may prevent the expected lowering of the optical band gap between **1** and **2**. That being said, we do not have a more thorough understanding of this phenomena at this time. Solid-state photoluminescence shows moderate red-shifting of the emission peak for each compound compared to solution photoluminescence with the effect being greater for **2** than **1**. This larger change in the photoluminescent peak wavelength could be attributable to an increase in intermolecular interactions in the solid state afforded by the greater degree of conjugation.

Relative fluorescent quantum yield measurements were performed in THF and referenced to 9,10-diphenylanthracene in a cyclohexane solution ($\Phi_{yield} \approx 0.9$) [23]. The difference in solvents was necessitated by the low solubility

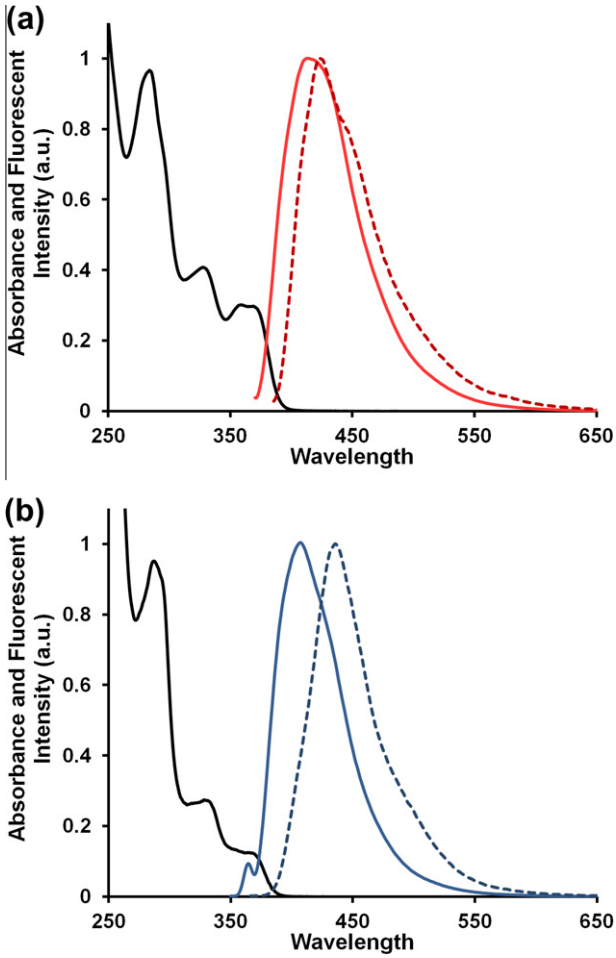


**Fig. 2.** Normalized absorption (black line) and emission spectra (solid colour for solution, dashed for thin film) of **1** (a) and **2** (b). Solution spectra were collected in THF.

**Table 1**
Photophysical, electrochemical and thermal properties of compounds **1** and **2**.

| Compound | $\lambda_{max}^{solemission}$ (nm)[a] | $\lambda_{max}^{filmemission}$, (nm) | $\Phi_{sol}$ (%)[a,b] | $E_{ox}^{peak}$ (onset) (V)[c] | $E_{red}^{peak}$(V)[c] | $E_{HOMO}$[d] [calculated][e] (eV) | $E_{LUMO}$[f] [calculated][e] (eV) | $T_d$ (°C)[g] |
|---|---|---|---|---|---|---|---|---|
| **1** | 410 | 421 | ~1 | 1.76 (1.56) | −1.62 | −6.14 [−6.07] | −2.93 [−2.14] | 277 |
| **2** | 405 | 434 | 0.9 | 1.66 (1.53) | – | −6.11 [−6.02] | −2.86 [−2.15] | 396 |

[a] Measured in tetrahydrofuran; $\lambda_{excitation}$ = 340 nm.
[b] Measured relative to 9,10-diphenylanthracene in cyclohexane [23].
[c] Peak and onset potential versus Ag/AgCl.
[d] Estimated from onset potential [24].
[e] As determined from DFT calculations.
[f] Estimated from HOMO and optical bandgap.
[g] Defined as 5% mass loss from TGA.

of **1** and **2** in cyclohexane. 9,10-Diphenylanthracene was chosen as a reference as it has similar absorbance and emission wavelengths as our compounds. Solutions were degassed prior to each experiment and sufficiently low concentrations were used to minimize reabsorption errors. Both compounds are highly photoluminescent with **1** having a quantum yield of near unity while **2** having a quantum yield of 0.9. The high photoluminescent efficiencies were surprising as phthalonitriles are not known to be particularly efficient fluorophores. To the best of our knowledge this is the first examples of strongly fluorescent phthalonitrile derivatives.

In order to explore the potential of these compounds to be used as emitters in OLEDs, each was characterized by solution electrochemical techniques and thermogravimetric analysis. The electrochemical behaviour of **1** and **2** was

determined through cyclic voltammetry in dichloromethane with 0.1 M of tetrabutylammonium perchlorate as a supporting electrolyte. Both compounds displayed fully irreversible oxidation waves with peak potentials at 1.76 and 1.66 V vs. Ag/AgCl for **1** and **2**, respectively (Table 1). Additionally, an irreversible reduction peak is observed for compound 1 at −1.62 V vs. Ag/AgCl while no clear reduction activity was observed for **2**. From this data, absolute molecular orbital energies were estimated [24] from the onset oxidations waves for the HOMO energy, while the LUMO energy values were estimated from the HOMO energy added to the energy of the optical bandgap (Table 1).

Most OLED layers are deposited using physical vapour deposition requiring candidate compounds to possess some degree of thermal stability in order to be processed into devices. To evaluate the compatibility of phthalonitriles **1** and **2** with modern OLED manufacturing techniques, the thermal stability of each was measured using thermogravimetric analysis (TGA) under $N_2$ with a ramp rate of 10 °C/min. For compounds **1** and **2** we observed a 5% mass loss at 277 and 396 °C (Table 1), respectively. A complete loss of initial mass was observed for compound **1** indicating no formation of ash. This implies that the compound simply sublimed upon heating. In the case of phthalonitrile **2**, ash was formed and thus the 5% weight loss indicates the onset of decomposition of the compound. Regardless of the nature of the 5% weight loss, these relatively high values confirm the stability of these structural motifs and suggest that they would be well-suited for physical vapour deposition.

Alluded to above, geometry optimized DFT calculations were performed not only to understand the molecular shape and conformation of **1** and **2** but also to aid the understanding of electronic structure of this structural motif. Because compounds **1** and **2** represent a completely new class of fluorophore, an understanding of the electronic structure is important for further elaboration on the molecular structure. Visualizations of the calculated HOMO and LUMO are given in Fig. 1. In each case, the HOMO is evenly distributed throughout the entire conjugated structure of the molecules. In contrast, the LUMO is isolated to the phthalonitrile core of each

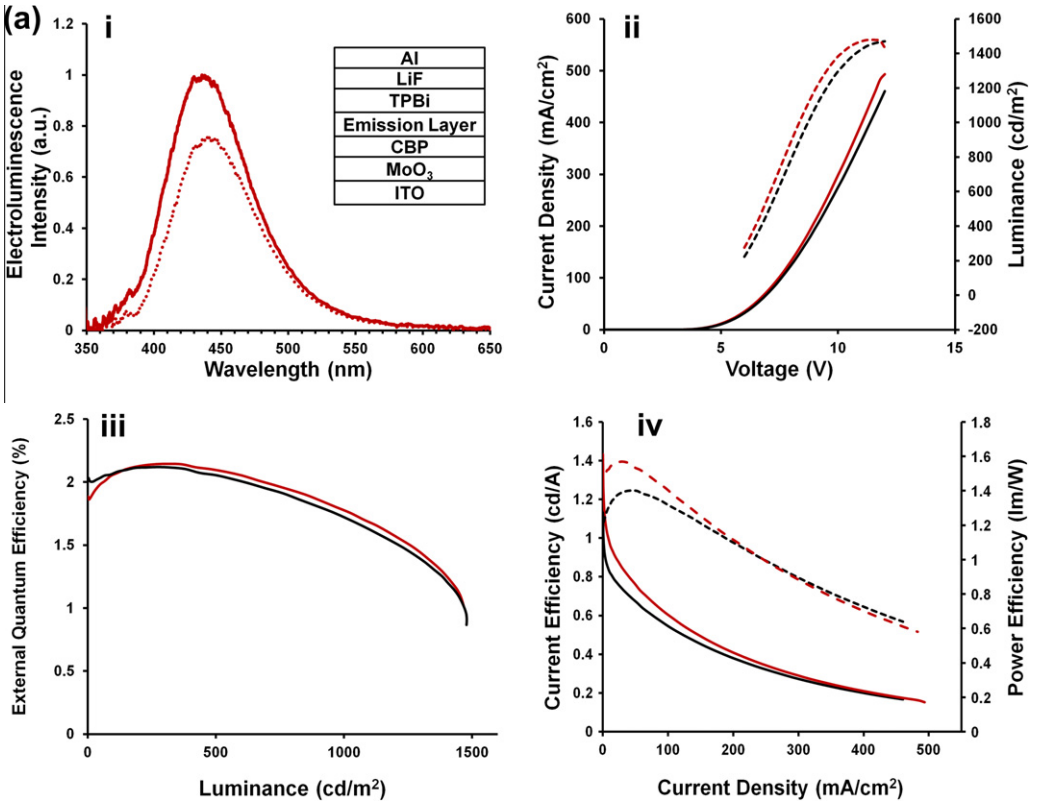


**Fig. 3.** (a) (i) Electroluminescent spectra of compound **1** (solid lines are for 2 wt.% doping in the emission layer and hashed lines are for 4 wt.% doping) at 100 cd/m$^2$; (ii) current density (solid lines) and luminance (hashed lines) as a function of voltage for devices using 2 wt.% (black lines) and 4 wt.% (red lines) of compound **1** as a dopant in the emission layer; (iii) external quantum efficiency versus luminance for devices using 2 wt.% (black line) and 4 wt.% (red line) compound **1** as a dopant in the emission layer; (iv) current efficiency (hashes lines) and power efficiency (solid lines) as a function of current density in devices using 2 wt.% (black lines) and 4 wt.% (red lines) compound **1** as a dopant in the emission layer. Device architecture for all devices is illustrated (a(i), inset). (b) (i) Electroluminescent spectra of compound **2** (solid lines are for 2 wt.% doping in the emission layer and hashed lines are for 4 wt.% doping) at 100 cd/m$^2$; (ii) current density (solid lines) and luminance (hashed lines) as a function of voltage for devices using 2 wt.% (black lines) and 4 wt.% (blue lines) of compound **2** as a dopant in the emission layer; (iii) external quantum efficiency versus luminance for devices using 2 wt.% (black line) and 4 wt.% (blue) compound **2** as a dopant in the emission layer; (iv) current efficiency (hashes lines) and power efficiency (solid lines) as a function of current density in devices using 2 wt.% (black lines) and 4 wt.% (blue lines) compound **2** as a dopant in the emission layer. Device architecture for all devices is illustrated (a(i), inset). (For interpretation of the references to colour in this figure legend, the reader is referred to the web version of this article.)

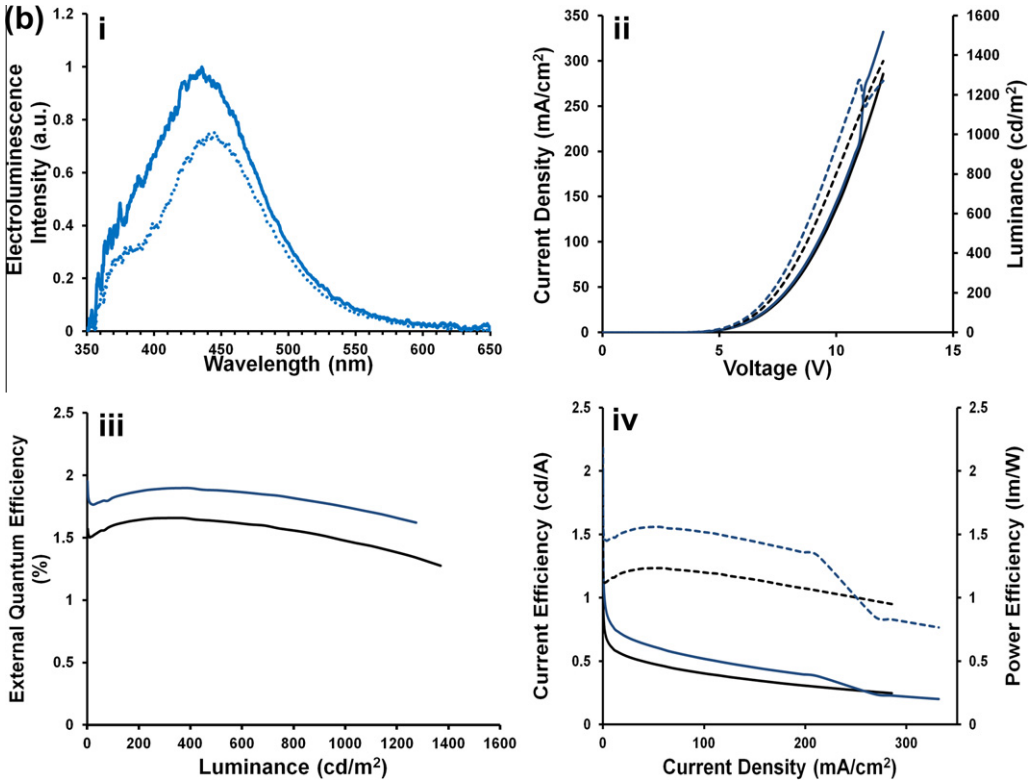


**Fig. 3** (*continued*)

molecule. This distribution of orbital densities suggests that tuning of the HOMO could easily be accomplished by the addition of electron donating groups to the periphery of the molecules whereas little variation would be possible in the LUMO level.

Finally, each molecule was incorporated as a fluorescent dopant in a series of four simple OLED devices [25] at both 2 and 4 wt.% with respect to the host material (4,4′-di(9-carbazolyl)-biphenyl, CBP) (Fig. 3, Table 2). The device structure used was: ITO/$MoO_3$/CBP (35 nm)/emitting layer (15 nm)/TPBi (65 nm)/LiF (1 nm)/Al (100 nm) where the emitting layer is composed of the fluorescent dopant and CBP (TPBi = 2,2′,2″-(1,3,5-benzinetriyl)tris(1-phenyl-1-H-benzimidazole)). All four devices achieved deep-blue emission with CIE coordinates that are exceptionally close to standard blue ($CIE_x$ = 0.14, $CIE_y$ = 0.08) with moderate luminance values and good turn-on voltages (Fig. 3). In particular, devices made using **1** showed blue emission that comes very close to the ideal value with CIE coordinates of $CIE_x$ = 0.16, $CIE_y$ = 0.08 (for the 2 wt.% doped device at 100 cd/m$^2$). Looking at the electroluminescent spectra for compound **1** (Fig. 3), we can conclude that there is almost exclusively emission from the dopant with a small shoulder at wavelengths <400 nm. For devices using **2** however, significant emission occurred below 400 nm and a broadened peak shape was observed. This shoulder is consistent with electroluminescence from the CBP host material [26] and either implies poor charge balance within the device, or inefficient energy transfer from the host to the dopant. Moreover, when comparing the estimated energy levels of the fluorophores to that of the host material (CBP) using the same methods as above, CBP has a significantly higher HOMO level at −5.61 eV [27]. This large mismatch in the HOMO energies of the host and guest may impede direct energy trapping by the guest molecule resulting in endothermic energy transfer and ultimately limit the efficiency of the devices. The observation that the electroluminescence from the host material appears more prominent for compound **2** compared to compound **1** could be attributable to the higher $E_{lumo}$ of −2.86 eV for compound **2** as

**Table 2**
Performance of OLEDs incorporating **1** and **2** as dopants.

| Compound | Concentration (wt.%) | $V_{turn\ on}$ (V)[a] | $EQE_{max}$ (%) | $\lambda_{max}^{EL}$(nm)[b] | $CIE_x$[b] | $CIE_y$[b] |
|---|---|---|---|---|---|---|
| 1 | 2 | 3.4 | 2.14 | 434 | 0.16 | 0.08 |
| | 4 | 3.4 | 2.12 | 440 | 0.16 | 0.09 |
| 2 | 2 | 3.8 | 1.66 | 434 | 0.16 | 0.11 |
| | 4 | 3.8 | 1.90 | 444 | 0.16 | 0.12 |

[a] As defined by a luminance of >0.5 cd/m$^2$.
[b] Determined at a luminance of 100 cd/m$^2$.

compared to that of compound **1** (−2.93 eV, Table 1). This could lead to a lower capability for the CBP host to confine charges to compound **2**, leading to a higher probability of energy back transfer from the dopant to the host thereby resulting in higher host emission.

Despite the potential challenges in device optimization, these initial prototype devices performed admirably well. A maximum external quantum efficiency of 2.14% was observed for the 2 wt.% doped device with compound **1** while devices made with compound **2** showed slightly lower values with a maximum of 1.90%. Both values are extremely promising and we anticipate that further engineering of the devices and the compounds themselves can yield even higher performance. Lifetime measurements were prevented by the low morphological stability of the host material, CBP with low glass transition temperature of ~62 °C [28]. Future development of more stable hosts and transport layers are in progress to study device life times.

## 4. Conclusions

In summary, we have synthesized and characterized two novel phthalonitrile based fluorophores for use in deep-blue OLEDs that approach the NTSC standard for blue. The compounds possess many ideal qualities for use in OLED devices including good emission coordinates/colour and thermal stability. When incorporated into prototype OLEDs, these compounds undergo electroluminescence with high external efficiencies and a colour near the NTSC standard for blue. The high efficiency and good colour rendering of these compounds suggests that they may be a promising material for application in a full colour OLED display.

## References

[1] S.R. Forrest, Nature 428 (2004) 911.
[2] CIE Commission Internationale de l'Eclairage Proceedings, Cambridge University Press: Cambridge, 1932.
[3] D.G. Fink, Color Television Standards: Selected Papers and Records, McGraw-Hill, New York, 1955.
[4] H. Sasabe, E. Gonmori, T. Chiba, Y.-J. Li, D. Tanaka, S.-J. Su, T. Takeda, Y.-J. Pu, K.-i. Nakayama, J. Kido, Chem. Mater. 20 (2008) 5951.
[5] N. Chopra, J. Lee, Y. Zheng, S.-H. Eom, J. Xue, F. So, Appl. Phys. Lett. 93 (2008) 143307.
[6] I.R.d. Moraes, S. Scholz, B. Lussem, K. Leo, Org. Electron. 12 (2011) 341.
[7] S.O. Jeon, K.S. Yook, C.W. Joo, J.Y. Lee, Adv. Mater. 22 (2010) 1872–1876.
[8] S.O. Jeon, S.E. Jang, H.S. Son, J.Y. Lee, Adv. Mater. 23 (2011) 1411–1436.
[9] H. Sasabe, J. Takamatsu, T. Motoyama, S. Watanabe, G. Wagenblast, N. Langer, O. Molt, E. Fuchs, C. Lennartz, J. Kido, Adv. Mater. 22 (2010) 5003–5007.
[10] Y. Sun, N.C. Giebink, H. Kanno, B. Ma, M.E. Thompson, S.R. Forrest, Nature 440 (2006) 908.
[11] T.C. Rosenow, M. Furno, S. Reineke, S. Olthof, B.R. Lussem, K. Leo, J. Appl. Phys. 108 (2010) 113113.
[12] M.T. Lee, C.H. Liao, C.H. Tsai, C.H. Chen, Adv. Mater 17 (2005) 2493.
[13] M.-H. Ho, Y.-S. Wu, S.-W. Wen, T.-M. Chen, C.H. Chen, Appl. Phys. Lett. 91 (2007) 083515.
[14] S.-K. Kim, B. Yang, Y. Ma, J.-H. Lee, J.-W. Park, J. Mater. Chem. 18 (2008) 3376.
[15] S.O. Kim, K.H. Lee, G.Y. Kim, J.H. Seo, Y.K. Kim, S.S. Yoon, Synth. Met. 160 (2010) 1259.
[16] M.-H. Ho, Y.-S. Wu, S.-W. Wen, M.-T. Lee, T.-M. Chen, C.H. Chen, K.-C. Kwok, S.-K. So, K.-T. Yeung, Y.-K. Cheng, Z.-Q. Gao, Appl. Phys. Lett. 89 (2006) 252903.
[17] S. Tao, Y. Zhou, C.-S. Lee, X. Zhang, S.-T. Lee, Chem. Mater. 22 (2010) 2138.
[18] S.-H. Liao, J.-R. Shiu, S.-W. Liu, S.J. Yeh, Y.-H. Chen, C.-T. Chen, T.J. Chow, C.-I. Wu, J. Am. Chem. Soc. 131 (2008) 763.
[19] S.J. Lee, J.S. Park, K.-J. Yoon, Y.-I. Kim, S.-H. Jin, S.K. Kang, Y.-S. Gal, S. Kang, J.Y. Lee, J.-W. Kang, S.-H. Lee, H.-D. Park, J.-J. Kim, Adv. Funct. Mater. 18 (2008) 3922.
[20] I. Noviandri, K.N. Brown, D.S. Fleming, P.T. Gulyas, P.A. Lay, A.F. Masters, P. Leonidas, J. Phys. Chem. B 103 (1999) 6713–6722.
[21] A.D. Becke, Phys. Rev. A 38 (1988) 3098–3100.
[22] P. Gregory, S.J. Reynolds, US Patent 6, 335(2002)442.
[23] D.F. Eaton, Pure Appl. Chem. 60 (1988) 1107.
[24] C.M. Cardona, W. Li, A.E. Kaifer, D. Stockdale, G.C. Bazan, Adv. Mater. 23 (2011) 2367.
[25] Z.B. Wang, M.G. Helander, J. Qiu, D.P. Puzzo, M.T. Greiner, Z.W. Liu, Z.H. Lu, Appl. Phys. Lett. 98 (2011) 073310.
[26] L. Zou, V. Savvate'ev, J. Booher, C.H. Kim, J. Shinar, Appl. Phys. Lett. 79 (2001) 2282.
[27] D. Hu, P. Lu, C. Wang, H. Lie, H. Wang, Z. Wang, T. Fei, X. Gu, Y. Ma, J. Mater. Chem. 19 (2009) 6143.
[28] L. Xiao, Z. Chen, B. Qu, J. Luo, S. Kong, Q. Gong, J. Kido, Adv. Mater. 23 (2011) 926.